Picosecond Time-Resolved Resonance Raman Study of the Solvated Electron in Water

Misao Mizuno and Tahei Tahara*

Molecular Spectroscopy Laboratory, The Institute of Physical and Chemical Research (RIKEN), 2-1 Hirosawa, Wako 351-0198, Japan

Received: September 9, 2002; In Final Form: January 15, 2003

Picosecond time-resolved Raman spectra of water were measured under the resonance condition with the electronic transition of the solvated electron. Transient Raman bands were observed in the OH bend and the OH stretch regions in accordance with the generation of the solvated electron. The lifetimes of the transient Raman bands were shortened by the addition of the electron scavenger, in exactly the same manner as the solvated electron absorption. It was concluded that the observed transient Raman bands are attributed to the water molecules that directly interact with the electron in the first solvation shell. The resonance enhancement factors were estimated as high as $\sim 10^5$ (the OH bend) and $\sim 10^3$ (the OH stretch) when the probe wavelength was tuned to the absorption maximum of the s → p transition of the solvated electron. The observed very high resonance enhancement indicated that the vibrational state of the solvating water molecules is strongly coupled with the electronic state of the electron. This implied that we should consider the electron and the solvating water molecules together (as a "quasi-molecule") when we discuss the vibronic state of the local solvation structure. The probe wavelength dependence of the transient Raman intensity was examined in a wide range from 410 to 800 nm. The obtained excitation profiles suggested that the s → conduction transition does not significantly contribute to the resonance Raman enhancement. The polarized Raman measurement was also undertaken for the OH bend band. A nonzero depolarization ratio was observed, which showed that the nondegeneracy of the three sublevels in the excited p state can be observed on the time scale of the Raman process. The OH bending and OH stretching frequencies of the solvating water molecule are downshifted compared with the frequencies of the bulk water, indicating that a structural change is induced by the strong interaction with the electron.

1. Introduction

The solvated electron in water has been attracting much interest in wide fields in chemistry, physics, and biology because of its fundamental importance. A large number of spectroscopic studies have been carried out since the optical absorption of the solvated electron was measured in water by pulse radiolysis.[1] It is well-known that the solvated electron in water exhibits a very broad absorption band peaked around 720 nm. It has an asymmetric shape that is well fitted with a combination of the Gaussian ($\lambda > \lambda_{max}$) and Lorentzian ($\lambda < \lambda_{max}$) functions.[2] The theoretical calculation indicated that the ground state and the first excited state of the solvated electron are the s-like and the p-like states, respectively, and that the broad absorption is mainly attributed to the s → p transition of the electron in a solvent cavity.[3,4] The solvated electron can also be created by the laser flash photolysis,[5,6] and the ultrafast dynamics of the solvated electron has been studied by femtosecond time-resolved absorption spectroscopy.[7−15] The spectral evolution after the photoionization of water as well as seed molecules was studied by using two-pulse sequences, whereas the dynamics after excitation of the thermally equilibrated solvated electron was examined with three-pulse sequences. The formation/relaxation mechanisms of the solvated electron were intensively discussed on the basis of the time-resolved absorption data, but they are still controversial. Recently, it was pointed out that the solvation dynamics of the electron significantly depends on the initial degree of the electron delocalization.[11]

In order to understand the physicochemical properties of the solvated electron in water, the information about the local solvation structure is obviously indispensable. Keavan studied the electron in low-temperature water matrixes by ESR spectroscopy, and concluded that the solvated electron is surrounded by six water molecules that are arranged octahedrally.[16] The structure of the water cluster anions in the gas phase have also been studied experimentally and theoretically, as a model of the solvated electron in water.[17−21] These works provided important information about the local solvation structure as well as the interaction between the electron and the water molecule. However, direct information about the local solvation structure is still scarce in the condensed phase, especially for the solvated electron at room temperature.

Very recently, we measured picosecond time-resolved Raman scattering from water under the resonance condition with the electronic transition of the solvated electron. We found, for the first time, that strong transient Raman bands appeared in accordance with the generation of the solvated electron. The observed transient Raman scattering was assigned to the water molecules that directly interact with the electron.[22] Shortly after our first paper, the same phenomenon was also reported by Tauber and Mathies, who independently carried out experiments using nanosecond lasers.[23,24] The observation of resonance Raman scattering from the "solvated electron" suggested that the local solvation structure around the electron can be directly studied by vibrational spectroscopy. Thus, vibrational spectroscopy is now expected to afford unique data that shed new light on the property of the solvated electron in water.

---

* Author to whom correspondence should be addressed. Fax: +81-48-467-4539. E-mail: tahei@postman.riken.go.jp.

10.1021/jp022030p CCC: $25.00

In this paper, we present a full account of our picosecond time-resolved Raman study of the solvated electron in water. We describe transient Raman bands observed in the OH bend and OH stretch regions, and confirm our assignment by the effect of the electron scavenger. The mechanism of this novel resonance enhancement is considered on the basis of the vibronic theory of the resonance Raman scattering. We examine the probe wavelength dependence of the transient Raman intensity and also discuss the data of the polarization measurements. The downshifted OH bending and OH stretching frequencies of the solvating water molecules are discussed in relation to the local structure around the electron.

2. Experimental Section

The experimental setup for picosecond time-resolved Raman measurements has been already described elsewhere.[25,26] Briefly, a picosecond mode-locked Ti:sapphire laser (Spectra-Physics, Tsunami) pumped by an Ar^+ ion laser (Spectra-Physics, Beamlok 2060-10SA) was used as the light source of the apparatus. The output of this oscillator laser was amplified by a regenerative amplifier (Spectra-Physics, Spitfire) with a cw Q-switched Nd:YLF laser (Spectra-Physics, Merlin). The pulse width, energy, and repetition rate of the amplified pulse were 2 ps, 600 μJ, and 1 kHz, respectively. The wavelength was changed from 770 to 840 nm by tuning the color of the oscillator laser. The second harmonic of the amplified pulse was generated by a 5-mm LBO crystal, and then the third harmonic was created by a 5-mm BBO crystal. Six wavelengths, 410, 494, 620, 770, 800, and 810 nm, were used for probing transient resonance Raman scattering. The 770-nm, 800-nm, and 810-nm pulses were the fundamental output of the Ti:sapphire laser. The 410-nm pulse is the second harmonic of the laser output. The 494-nm (the first Stokes line) and 620-nm (the second Stokes line) pulses were generated from a H_2 Raman shifter that was excited by the second harmonic (410 nm). The third harmonic pulses (273 nm for the 410-, 494-, and 620-nm probe, 257 nm for the 770-nm probe, 267 nm for the 800-nm probe, 270 nm for the 810-nm probe) of the amplified pulse were used for the photoexcitation to generate solvated electrons in water.

The pump and probe pulses were focused by a quartz lens ($f = 50$ mm) onto a thin film-like jet stream (thickness ∼ 300 μm) of the sample solution. Typical pulse energy is 20−25 μJ (pump) and 1−10 μJ (probe) at the sample point. Typical cross correlation time between the pump and probe pulses was about 5 ps (fwhm). The Raman scattering was collected and introduced into a spectrometer (Jobin-Yvon, HR320) using a camera lens. A holographic notch filter (Kaiser Optical Systems, Inc.) or sharp-cut colored glass filters (HOYA) were used to eliminate Rayleigh scattering. A liquid nitrogen cooled CCD camera (Princeton Instruments, LN/CCD-1100PB) was used for the detection of Raman scattering in the visible region, whereas a liquid nitrogen cooled InGaAs array detector (Jobin-Yvon, IGA-512 × 1-1) was used for the near-infrared Raman detection. Time-resolved absorption was measured by monitoring the intensity of the probe pulse that passed through the sample.

Indole (special grade) was purchased from Tokyo Chemical Industry Co., Ltd. and sublimated in vacuo. Potassium ferrocyanide trihydrate (special grade) was purchased from Wako Pure Chemical Industries and used without purification. Water was distilled and deionized before use. Acetonitrile (HPLC grade) and acetone (special grade) were purchased from Wako Pure Chemical Industries and used as received.

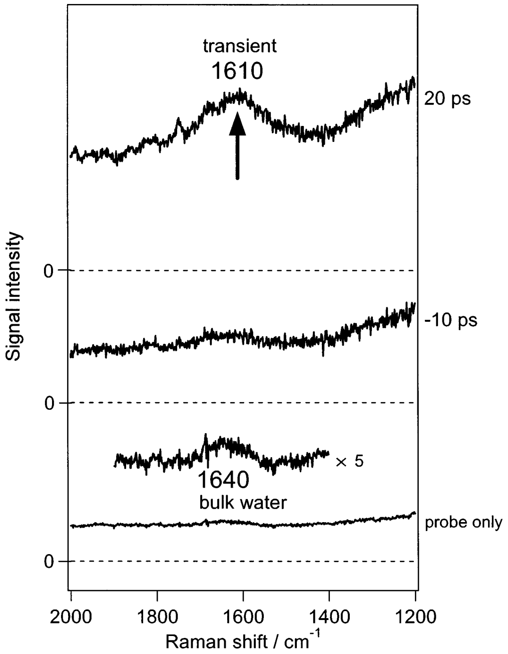

Figure 1. Picosecond time-resolved resonance Raman spectra in the OH bend region of water in the presence of indole (1.7 × 10^{-3} mol dm^{-3}; pump laser, 267 nm; probe laser, 800 nm). Spectrum taken with only pump pulse irradiation has been subtracted from each time-resolved spectrum.

3. Results and Discussion

3.1. Observation of Transient Resonance Raman Scattering in the OH Bend Region. Figure 1 shows picosecond time-resolved resonance Raman spectra of water in the OH bend region measured with the 800-nm probe. This probe wavelength is close to the maximum of the transient absorption of the solvated electron in water. Indole was added to water as a seed molecule for efficient generation of the solvated electron. The spectrum taken with pump pulse irradiation has been already subtracted from the time-resolved spectra shown in this figure. In the spectrum taken before the pump irradiation (−10 ps), as well as in the spectrum measured with only probe pulse irradiation, only a weak Raman band due to the OH bending vibration of the bulk water was observed at ∼1640 cm^{-1}. After the pump irradiation, a strong transient Raman band appeared on a featureless luminescence signal in accordance with the generation of the solvated electron. The peak frequency of the transient Raman band is ∼1610 cm^{-1}, which is ∼30 cm^{-1} lower than the OH-bending frequency of the bulk water. We also measured time-resolved Raman spectra from neat water as well as water in the presence of other seed molecules (KI, etc.). We observed the same transient Raman band in all cases. Therefore, the transient species that gives rise to this transient Raman band was safely attributed to a water transient, not to the transient species produced from the seed molecule. The featureless luminescence signal observed with the transient Raman band is assigned to the fluorescence of the solvated electron.[23]

The time-resolved spectra shown in Figure 1 indicate that the observed water transient species gains high Raman intensity enhancement under the resonance condition with the electronic transition of the solvated electron. However, in the time-resolved resonance Raman measurements, it is difficult to quantitatively compare the intensity of Raman band measured at different delay times, because Raman scattering is re-absorbed by the sample that exhibits transient absorption. In the present experiment, it was also necessary to ensure that the optical artifacts such as thermal effects did not affect the time-resolved Raman spectra.

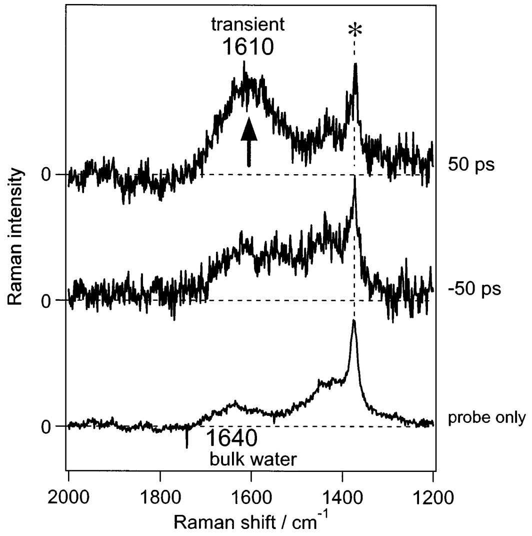

Figure 2. Picosecond time-resolved resonance Raman spectra in the OH bend region of a water−acetonitrile mixture (4:1) in the presence of indole (1.7×10^{-3} mol dm^{-3}; pump laser, 267 nm; probe laser, 800 nm). The Raman intensity at each delay time has been normalized by using the acetonitrile band intensity. The spectrum taken with only pump pulse irradiation and luminescence signal arising from probe pulse irradiation has been subtracted from each time-resolved spectrum. The Raman band of acetonitrile is indicated by an asterisk.

Thus, we carried out time-resolved Raman measurements of a water−acetonitrile mixture (4:1). It has been reported that the solvated electron is not formed in acetonitrile,[27] so that the Raman bands of acetonitrile do not change with the generation of the solvated electron. Therefore, the acetonitrile Raman bands can be used as the intensity standard, and the Raman intensity in time-resolved spectra can be quantitatively compared after intensity normalization. (For this reason, we often use a water−acetonitrile mixture in the experiments described in this paper.) The intensity-normalized time-resolved Raman spectra obtained from a water−acetonitrile mixture are shown in Figure 2. The same transient Raman band was observed at the same position (~1610 cm^{-1}) as observed in the time-resolved spectra of water. The intensity of the transient Raman band was about 4 times larger than that of the bulk water despite the low concentration of the transient species (vide infra), which confirmed that the water transient Raman band gains very high resonance enhancement through the electronic transition of the solvated electron.

The observed high resonance enhancement indicates that there exists a strong coupling between the water transient and the electron. In other words, the transient species giving rise to the strong resonance Raman band is attributable to the water molecule that strongly interacts with the electron.

In order to confirm this assignment, we examined the temporal behavior of the observed transient Raman band in the presence of an electron scavenger. Although the lifetime of the solvated electron is as long as a few hundred nanoseconds in pure water,[5] it is significantly shortened in the presence of the electron scavenger. For example, it is known that acetone efficiently quenches the solvated electron by the following reaction:[28]

$$CH_3COCH_3 + e^{\bullet -}_{aq} \rightarrow CH_3\dot{C}OCH_3^{\ -}$$

We added acetone to the sample and compared the effect on the temporal behaviors of the transient Raman and transient absorption intensities.

We measured time-resolved Raman spectra of a water−acetonitrile mixture in the presence of 1% acetone. Figure 3 shows the obtained picosecond time-resolved resonance Raman spectra in the OH bend region. The luminescence background has been subtracted from each time-resolved Raman spectrum, and the Raman intensity at each delay time has been normalized with use of the acetonitrile Raman band intensity. As marked by arrows, the transient Raman band was observed. However, in the presence of acetone, the transient Raman band decayed within a few nanoseconds. In Figure 4, the temporal change of the intensity of the transient Raman band at ~1610 cm^{-1} is compared with the decay of the transient absorption at 800 nm. As clearly seen, the temporal change of the transient Raman band is in very good agreement with that of the transient absorption, and they show a rapid decay with a lifetime of as short as 1.2 ns. For comparison, the temporal behavior in the absence of acetone is also shown in Figure 4b. Reflecting the long lifetime of the solvated electron without any scavenger, both of the transient Raman and absorption signals did not show any noticeable decay in the time range of the present measurements. These results clearly demonstrated that the transient Raman band is quenched by the electron scavenger in exactly the same manner as the solvated electron. This shows that the relevant water transient certainly appears and disappears in accordance with the solvated electron.

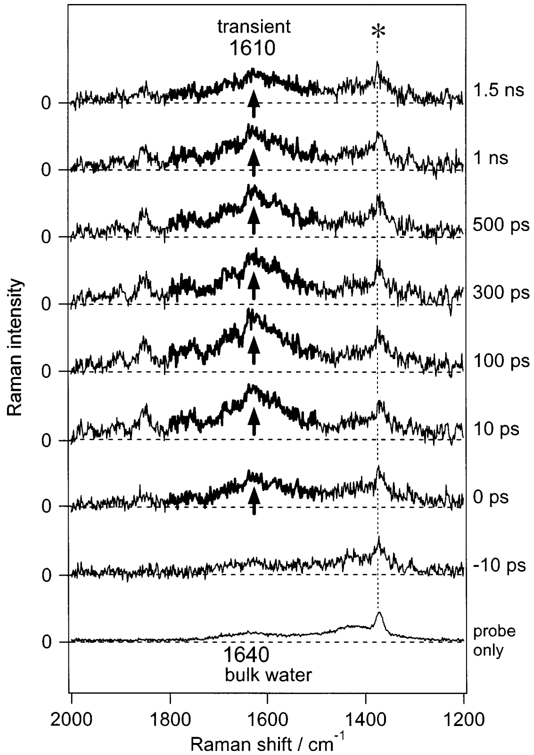

Figure 3. Picosecond time-resolved resonance Raman spectra in the OH bend region of a water−acetonitrile mixture (4:1) in the presence of indole (1.7×10^{-3} mol dm^{-3}) and 1% acetone (pump laser, 267 nm; probe laser, 800 nm). The Raman intensity at each delay time has been normalized by using the acetonitrile band intensity. The spectrum taken with only pump pulse irradiation and luminescence signal arising from probe pulse irradiation has been subtracted from each time-resolved spectrum. The Raman band of acetonitrile is indicated by an asterisk.

3.2. Observation of Transient Resonance Raman Scattering in the OH Stretch Region. Time-resolved Raman spectra in the OH stretch region could not be measured with the 800-nm probe using highly sensitive CCD, because the OH stretch band appears around 1.1 μm where CCD does not have sensitivity. Therefore, we carried out experiments using an InGaAs array detector for the OH stretch region. In contrast to the drastic change observed in the OH bend region, the spectral

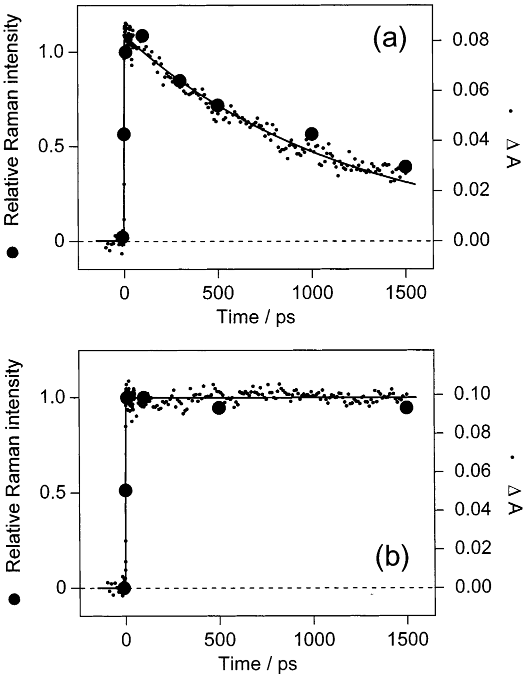

Figure 4. Temporal intensity change of the transient Raman band at 1610 cm^{-1} and transient absorption measured at 800 nm. (a) A water−acetonitrile mixture (4:1) in the presence of indole and 1% acetone, and (b) water in the presence of indole. Concentration of indole is 1.7 $\times$ 10^{-3} mol dm^{-3}. Temporal intensity change of Raman band have been normalized at the intensity measured at 10 ps. Large black circles indicate the intensity of transient Raman band at 1610 cm^{-1}. Small circles and solid lines exhibit the intensity of transient absorption and the best fitted curves, respectively.

change induced by the generation of the solvated electron was not very large in the OH stretch region. Actually, we needed to perform careful measurements to confirm the existence of the transient Raman band in this region. Figure 5a depicts picosecond time-resolved resonance Raman spectra of a water−acetonitrile mixture (4:1) probed at 800 nm. We show the spectra measured in the presence of acetone in order to discuss the temporal behavior of the spectral feature. Figure 5b shows the time-resolved spectra obtained after spectral subtraction. We subtracted the spectrum taken with only probe irradiation as well as the featureless fluorescence. Although the signal-to-noise ratio is not high, a weak transient Raman band is clearly recognized around 3170 cm^{-1}. This transient Raman band decays in a few nanoseconds in the presence of the electron scavenger (acetone), which indicates that this transient band is also attributable to the water molecule that interacts with the solvated electron. It should be noted that the acetonitrile Raman bands were completely erased in the subtracted spectra. It assured the validity of the subtraction procedure, and hence assured the existence of the transient Raman band observed in the OH stretch region.

The sensitivity of the InGaAs detector is lower than CCD, which made the signal-to-noise ratio of the spectra in the OH stretch region much lower. As described in Section 3.4, we also carried out picosecond time-resolved Raman measurements using shorter probe wavelengths. In such measurements, the OH stretch band of the water transient was detected with CCD. For comparison, the spectrum measured with the 620-nm probe is depicted in Figure 5c. A transient Raman band is clearly seen at the same position (~3170 cm^{-1}) as observed in the spectra measured with the 800-nm probe.

3.3. Assignment of the Water Transient and the Mechanism of the Intensity Enhancement.

The experiments described in the previous two sections showed that the observed transient Raman bands are attributed to the vibrations of the water transient that appears and disappears in accordance with the solvated electron. The frequencies of the two transient Raman bands (the OH bend and OH stretch bands) are lower than the frequencies of the corresponding Raman bands of the bulk water, which indicates that the structure of the water transient is somewhat different from that of water molecules in the bulk. These results strongly suggest that the observed water transient is ascribed to the water molecule that directly interacts with the solvated electron.

For the local structure around the solvated electron in water, Keavan studied the electron trapped in a low-temperature glass matrix.[16] On the basis of the ESR data, they concluded that six water molecules solvate the electron in the first solvation shell and that one of the OH bonds of each water molecule is oriented toward the electron. The distance between the center of the electron and the closest hydrogen atom was estimated to be ~0.2 nm. This local solvation structure was determined for a low-temperature matrix. At room temperature, it is expected that the solvation structure is fluctuated and not solid. Nevertheless, the averaged structure may be considered essentially similar. On the other hand, a molecular dynamics simulation indicated that the orbital radius of the ground s-state electron is ~0.2 nm,[3] and the electron is localized in a solvent cavity.[29] Since the orbital radius of the solvated electron is almost the same as the distance between the electron and the closest water molecule, it is natural to think that the water molecules in the first solvation shell interact with the electron much more strongly than those in the outer shell. Therefore, it is highly likely that the water transient observed in the time-resolved resonance Raman measurements is the water molecule in the first solvation shell around the electron. This argument is strongly supported by the experiments of water−acetonitrile mixtures described in the previous sections. In the presence of the high concentration of acetonitrile in solutions (which is added as the Raman intensity standard), the outer solvation shell is highly likely perturbed. Nevertheless, the Raman spectra of the water transients observed in the mixture do not show any noticeable change compared with those taken in neat water. Therefore, we can conclude that the vibrational spectra of the very local solvation structure around the electron are observed when we measure Raman scattering under the resonance condition with the absorption of the solvated electron.

It was surprising that the solvating water molecule gains high resonance Raman enhancement through the electronic transition of the electron. However, we consider that this intensity enhancement can be treated in the framework of the standard vibronic theory of the resonance Raman scattering,[30] if we deal with the electron and the solvating water molecules as a whole, in other words, as a “cluster” or a “quasi-molecule”.

In the frequency-domain representation, the intensity of the Raman scattering relevant to the $m \rightarrow n$ vibrational transition is represented as

$$I_{mn} = \frac{2^7\pi^5}{3^2c^4} I_0(\nu_0 - \nu_{mn})^4 \sum_{\rho,\sigma} |(\alpha_{\rho\sigma})_{mn}|^2$$

where

$$(\alpha_{\rho\sigma})_{mn} = \sum_r \left[\frac{\langle n|\mu_\rho|r\rangle\langle r|\mu_\sigma|m\rangle}{E_r - E_m - E_0 - i\Gamma} + \frac{\langle n|\mu_\sigma|r\rangle\langle r|\mu_\rho|m\rangle}{E_r - E_n + E_0 - i\Gamma} \right] \quad (1)$$

Here, $\alpha_{\rho\sigma}$ is the $\rho\sigma$th component of the Raman tensor; I_0 is the intensity of the incident light; E_0 is the photon energy of

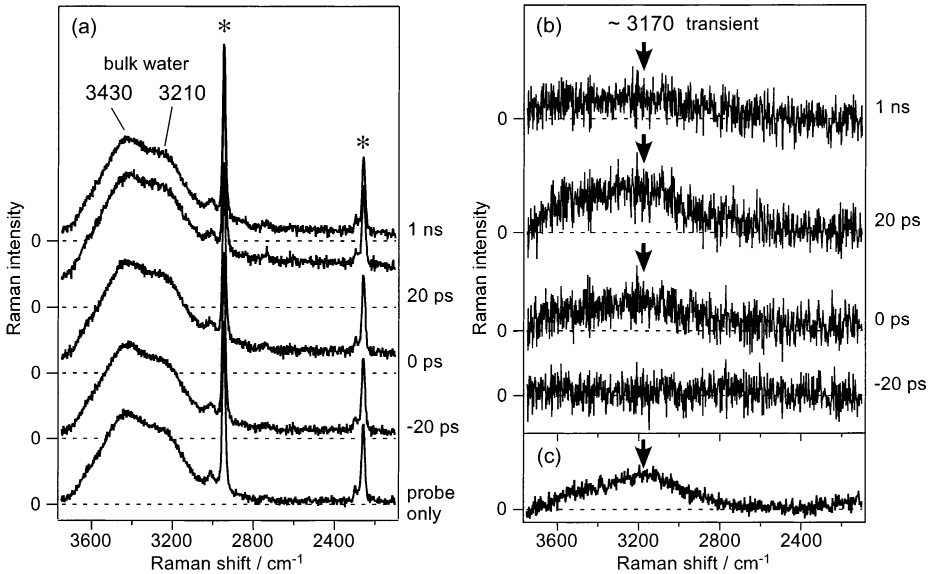

Figure 5. (a) Picosecond time-resolved resonance Raman spectra in the OH stretch region of a water−acetonitrile mixture (4:1) in the presence of indole (1.7×10^{-3} mol dm^{-3}) and 1% acetone (pump laser, 267 nm; probe laser, 800 nm). Raman intensity at each delay time has been normalized by using the acetonitrile band intensity. Spectrum taken with only pump pulse irradiation has been subtracted from each time-resolved spectrum. Asterisks indicate the Raman bands of acetonitrile. (b) Picosecond time-resolved resonance Raman spectra after the spectral subtraction. The luminescence signal arising from probe pulse irradiation and the acetonitrile Raman band were subtracted from (a). (c) Transient resonance Raman spectrum of a water−acetonitrile mixture (4:1) in the presence of ferrocyanide ion (5×10^{-3} mol dm^{-3}; pump laser, 273 nm; probe laser, 620 nm; delay time, 20 ps). The spectrum taken with only pump pulse irradiation and luminescence signal arising from probe pulse has been subtracted.

the incident light; ν_{mn} is the Raman shift ($= (E_n - E_m)/h$); m, n, and r are the initial, final, and intermediate states, respectively; μ_ρ is the ρth component of the electronic dipole moment operator. In the standard vibronic theory of the resonance Raman scattering, each state is expressed as the product of the electronic and vibrational wave functions (the Born−Oppenheimer approximation), and then the Raman tensor is expanded using the Herzberg−Teller expansion. The resultant zero-th and first order terms of the vibronic coupling are called as the A (the zero-th order) and B, C (the first order) terms. It is known that, in usual cases, the intensity enhancement of resonance Raman scattering is attributed to the A term (the Franck−Condon mechanism):

$$(\alpha_{\rho\sigma})_{gi,gj} \approx A + B + C\cdots \tag{2}$$

where

$$A \propto \sum_{e\neq g}{}' \sum_{v} \left[\frac{(g^0|\mu_\rho|e^0)(e^0|\mu_\sigma|g^0)}{E_{ev} - E_{gi} - E_0 - i\Gamma} \right] \langle j|v\rangle\langle v|i\rangle$$

As seen in this formula, the A term contains the Franck−Condon factor between the vibrational states in the ground and excited states. Therefore, in order that a particular vibrational mode gains high-intensity enhancement in the resonance Raman process, the vibrational states having different quantum number in the ground and excited states need to have a significant Franck−Condon factor. Thus, the potential curves of the ground and excited states need to be displaced along the relevant vibrational coordinate.

Concerning the resonance Raman scattering from the solvated electron, we treat the electron and the surrounding water molecules together. (For the sake of convenience, we call it the “solvated-electron cluster”.) Then, like an ordinary molecule, the vibronic states of the “solvated-electron cluster” can be expressed as the product of the electronic and vibrational wave functions:

$$\begin{aligned} |m\rangle &= |g_{\text{e-water}})|i\rangle \\ |n\rangle &= |g_{\text{e-water}})|j\rangle \\ |r\rangle &= |e_{\text{e-water}})|v\rangle \end{aligned} \tag{3}$$

Here, $g_{\text{e-water}}$ and $e_{\text{e-water}}$ represent the electronic ground and excited states of the “solvated-electron cluster”, respectively (Figure 6). In these formulas, the vibrational wave functions represent intra- and intermolecular vibrations of solvating water molecules. Since the excitation is localized in the electron at the center (and hence the electronic excitation of water molecules is negligible), the ground and excited states of the “solvated-electron cluster” are essentially the s and p states of the electron at the center. Then, the formula of the A-term resonance (eq 2) can be rewritten as follows:

$$\begin{aligned} A &\propto \sum_{v} \left[\frac{(g_{\text{e-water}}|\mu_\rho|e_{\text{e-water}})(e_{\text{e-water}}|\mu_\sigma|g_{\text{e-water}})}{E_{e_{\text{e-electron}},v} - E_{g_{\text{e-electron}},i} - E_0 - i\Gamma} \right] \langle j|v\rangle\langle v|i\rangle \\ &\approx \sum_{v} \left[\frac{(s^0|\mu_\rho|p^0)(p^0|\mu_\sigma|s^0)}{E_p - E_s - E_0 - i\Gamma} \right] \langle j|v\rangle\langle v|i\rangle \end{aligned} \tag{4}$$

Since the interaction between the electron and water molecules in the first solvation shell is very strong, it is expected that the vibrational states (or structure) of the solvating water molecules are significantly changed with the change of the electronic state of the solvated electron. In this case, as the formula (eq 4) indicates, a strong resonance Raman effect is expected for the vibrational modes of the solvating water molecules along which the structural change is induced with the electronic excitation of the electron.

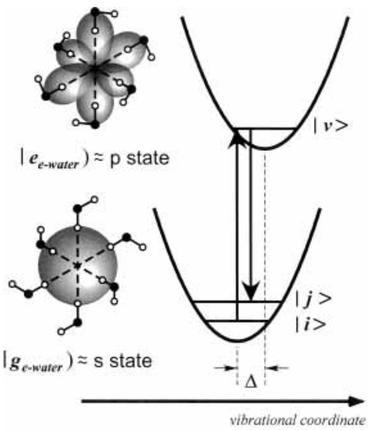

Figure 6. The vibronic states of the “solvated electron”.

The intensity of resonance Raman spectra provides information about the structural change induced with the electronic transition. In the resonance Raman spectra probed at 800 nm, the intensity of the OH bend band is highly enhanced, whereas the OH stretch band gains only moderate intensity enhancement. This indicates that the structural change, which is induced on the solvating water molecules by the s → p transition of the electron, is large along the OH bend coordinate but relatively small for the OH stretch coordinate.

3.4. Excitation Profiles: Probe Wavelength Dependence of Resonance Raman Intensity. The vibronic theory of resonance Raman scattering indicates that the intensity enhancement of Raman scattering is attributable not solely to the property of the ground state but also to the character of the electronic transition in resonance (the structural change induced by the electronic transition). Therefore, the resonance Raman intensity should significantly change when we change the electronic transition in resonance. Keeping this point in our mind, we examined the excitation (probe) wavelength dependence of the intensity of resonance Raman scattering from the solvated electron.

We measured picosecond time-resolved Raman spectra with four more probe wavelengths (410, 494, 620, 770 nm), and compared them with the spectra taken with the 800-nm probe. Five wavelengths, in total, cover almost the entire region of the broad absorption of the solvated electron. To obtain reliable excitation profiles, we did several things. First, we used a water−acetonitrile mixture as the sample in order to utilize the acetonitrile bands as the internal standard for the intensity normalization. Second, in the experiments using shorter wavelengths, we used potassium ferrocyanide ($K_4Fe(CN)_6$) as a seed molecule, in place of indole, because the cation radical of indole exhibits transient absorption around 580 nm. It is known that the ferrocyanide ion and its photooxidized products do not show any absorption in the visible wavelength region. Third, we set the probe intensity as low as possible to minimize the photobleaching of the ground-state solvated electron. Actually, a significant bleaching effect was observed in the experiment using the probe wavelength shorter than 500 nm.

The obtained time-resolved Raman spectra are shown in Figure 7 (the OH bend region) and Figure 8 (the OH stretch region).[31] We do not show the OH stretch region measured with the 770-nm probe, because the signal-to-noise ratio was very low. Either of the detectors, CCD or the InGaAs array, did not provide good data for the relevant wavelength region. For quantitative discussion, we calculated the enhancement factor of the transient Raman bands (the intensity ratio between the Raman scattering from a transient water molecule and that of a bulk water molecule) at each excitation wavelength by the following way. First, we compared the time-resolved spectra measured at 20 ps with the spectra taken with only probe irradiation, and evaluated the apparent intensity ratio ($R_I = I_{\text{transient}}/I_{\text{bulk}}$) between the water transient Raman band and the bulk water band. Second, we estimated the concentration of the solvated electron (c_{electron}) from the transient absorption intensity. For the estimation, we used the absorption coefficient of the solvated electron[2] and the optical path length of the sample solution, 300 μm. The concentration of the solvated electron varied in the range between 1.8×10^{-4} and 2.5×10^{-3} mol dm^{-3}, reflecting the difference in the experimental condition (the energy of the pump pulse, the focus size, etc.). Then, assuming that the number of the water molecules in the first solvation shell is also ~6 in water at room temperature ($N_{\text{solvation}} \cong 6$), the concentration of the water molecules that give rise to the transient Raman band was estimated. Since the concentration of the bulk water is readily obtained ($c_{\text{bulk water}} = 44$ mol dm^{-3} in the water−acetonitrile mixture), we can calculate the resonance enhancement factor, $f_{\text{resonance}}$, by using the following formula:

$$f_{\text{resonance}} = R_I \frac{c_{\text{bulk water}}}{N_{\text{solvation}} c_{\text{electron}}} \tag{5}$$

The resonance enhancement factor calculated for each probe wavelength is listed in Table 1 with the parameters used in the calculation. The excitation profiles are plotted in Figure 9 with the absorption spectrum of the solvated electron. We note that the ambiguity in $N_{\text{solvation}}$ might cause some error in the absolute value of the evaluated resonance enhancement factor. However, it does not affect relative values, so that it does not change the shape of the excitation profiles shown in Figure 9.

The obtained excitation profiles show that both of the vibrational bands, the OH bend and OH stretch bands, gain high-intensity enhancement when the probe wavelength is tuned around the maximum of the solvated electron absorption. The enhancement factor of the OH bend band becomes as large as $\sim 2 \times 10^5$. This enhancement factor is fairly large, even compared with the resonance Raman scattering from ordinary molecules. The enhancement factor of the OH stretch band is much smaller, but it is still as large as $\sim 4 \times 10^3$. A characteristic feature seen in the excitation profiles of the OH bend and OH stretch bands is that the resonance enhancement factor sharply decreases in the blue side of the absorption (<500 nm). Especially, the enhancement factor becomes very little at 400 nm, although the solvated electron still exhibits significant absorption.

The very small resonance enhancement in the blue side of the absorption is highly likely to reflect the difference in the nature of the electronic transition. The electronic state of the solvated electron in water was theoretically studied by Schnitker et al.[3] Their calculation showed that the energy of the p-type excited state is located just below the continuum (the conduction band, CB) and that the high-energy side of the p-state distribution is overlapped with the low-energy side of the conduction band. It implies that the blue side of the absorption of the solvated electron has a nature of the s → CB transition, although the major part of the absorption is attributable to the s → p transition. This conclusion of the theoretical calculation has been supported experimentally, for example, by recent femtosecond time-resolved absorption experiments of Barbara and coworkers.[12,13] They photoexcited the s state to the CB band with the 400-nm pulse and observed that geminate recombination is

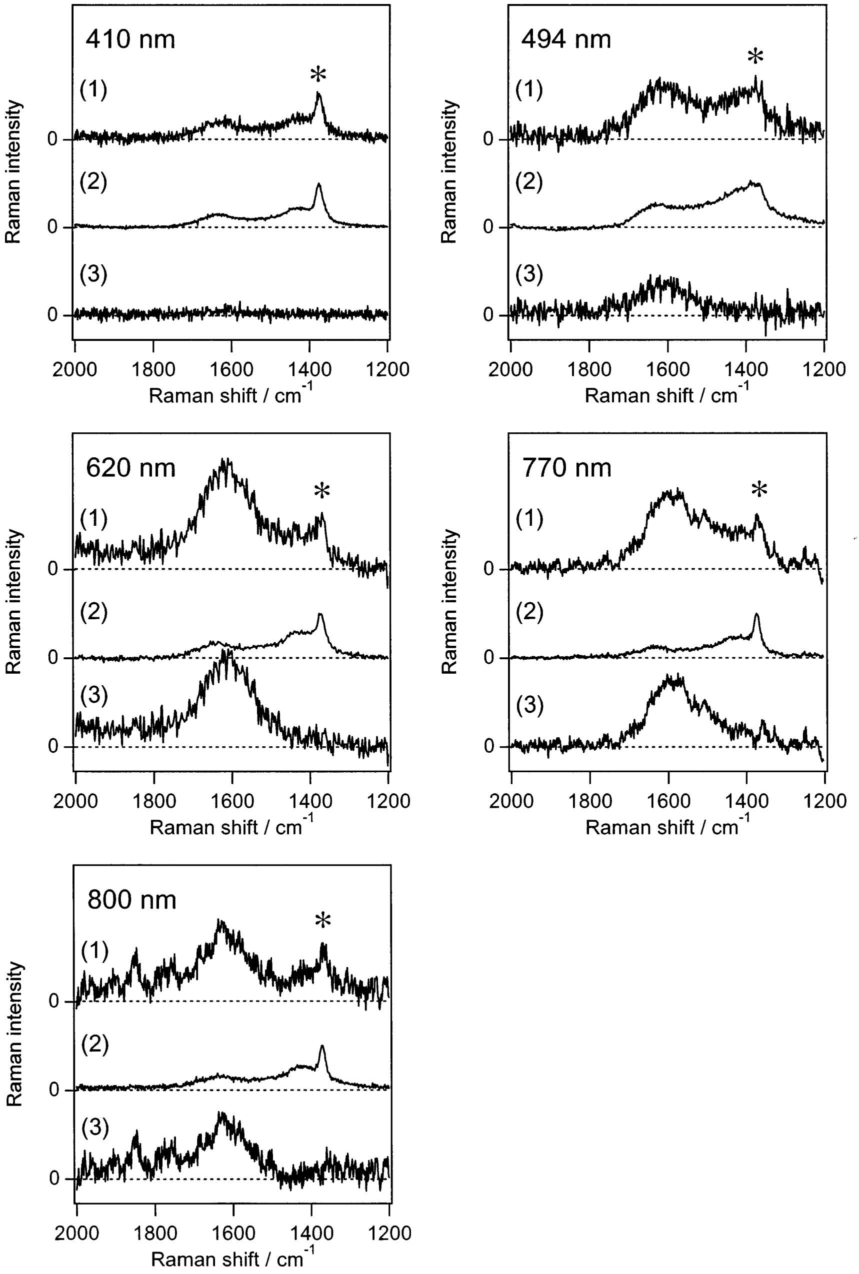

Figure 7. Raman spectra of a water−acetonitrile mixture (4:1) in the OH bend region. (1) Spectra measured at 20 ps delay time. Featureless luminescence signals were subtracted; (2) Spectra taken with only probe pulse irradiation; (3) Subtracted spectra, (1) − (2). The probe wavelength used for each experiment is indicated in the figure. Potassium ferrocyanide (5×10^{-3} mol dm^{-3}; 410−770-nm probe), or indole (1.7×10^{-3} mol dm^{-3}; 800-nm probe) was added as a seed molecule. Raman intensity has been normalized by using the intensity of the acetonitrile Raman band that is indicated by an asterisk.

suppressed owing to the de-trapping of the electron. Therefore, very small resonance Raman enhancement in the blue side of the absorption implies that the Raman scattering from the solvating water molecules are enhanced under the resonance condition with the s → p transition, but not with the s → CB transition. This conclusion is very consistent with the standard vibronic theory discussed in the previous section, because it is expected that the structural change induced by the s → CB transition is significantly different from that caused by the s → p transition.

3.5. Polarization Measurements: Nondegeneracy of the Sublevels of the p State. The present Raman study demonstrates that we should consider the electron and the solvating water molecules together as a “solvated-electron cluster” when we discuss the vibronic state of the local solvation structure. Nevertheless, the ground and excited states of the “solvated-electron cluster” is essentially the s and p states of the electron at the center. It is expected that the properties of the excited p state are strongly affected by the symmetry of local solvation structure, and it has been an issue of intense discussion.

The excited p state intrinsically has three sublevels, p_x, p_y, and p_z. If the system is isotropic, these three sublevels are degenerate, as the case of the 2p state of the hydrogen atom. However, a theoretical calculation based on the cavity model indicated that the p_x, p_y, and p_z states of the solvated electron are not degenerate because of the nonspherical nature of the solvent cavity. The energy splitting of the three sublevels was estimated as large as 0.8 eV.[3] This argument from the theory is widely accepted, but, as far as the authors know, it has not been well supported by the experiment. For example, Assel et al.

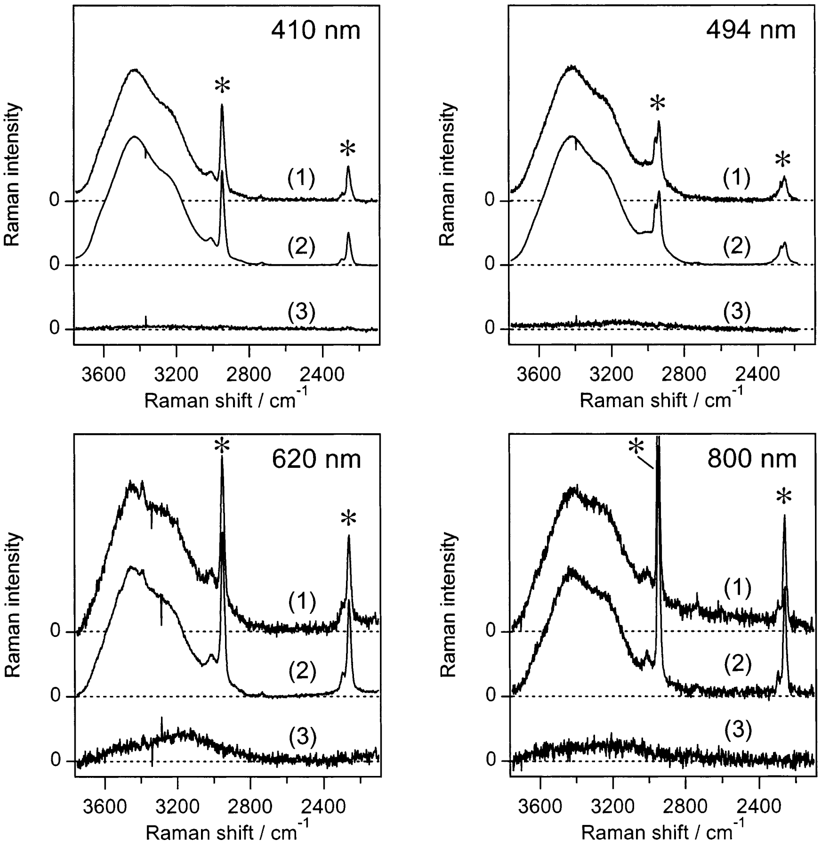

Figure 8. Raman spectra of a water−acetonitrile mixture (4:1) in the OH stretch region. (1) Spectra measured at 20 ps delay time. Featureless luminescence signals were subtracted; (2) Spectra taken with only probe pulse irradiation; (3) Subtracted spectra, (1) − (2). The probe wavelength used for each experiment is indicated in the figure. Potassium ferrocyanide (5×10^{-3} mol dm^{-3}; 410−620-nm probe), or indole (1.7×10^{-3} mol dm^{-3}; 800-nm probe) was added as a seed molecule. Raman intensity has been normalized by using the intensity of the acetonitrile Raman bands that are indicated by asterisks.

TABLE 1: Resonance Enhancement Factor of the OH Bend and OH stretch Bands

probe wavelength [nm]	absorption coefficient[a] [dm^{-3} mol^{-1} cm^{-1}]	ΔA @ 20 ps	c_{electron}[b] [mol dm^{-3}]	R_I[c]	$f_{\text{resonance}}$[d]
		OH bend band (~1610 cm^{-1})			
410	2300	0.16	2.3×10^{-3}	0.25 ± 0.15	$(7.9 \pm 4.7) \times 10^{2}$
494	5200	0.26	1.7×10^{-3}	1.10 ± 0.12	$(4.8 \pm 0.5) \times 10^{3}$
620	14000	0.18	4.3×10^{-4}	5.42 ± 1.01	$(9.3 \pm 1.7) \times 10^{4}$
770	17200	0.17	3.3×10^{-4}	7.50 ± 2.00	$(1.7 \pm 0.4) \times 10^{5}$
800	15600	0.083	1.8×10^{-4}	5.02 ± 0.59	$(2.1 \pm 0.2) \times 10^{5}$
		OH stretch band (~3170 cm^{-1})			
410	2300	0.17	2.5×10^{-3}	0.005 ± 0.005	$(1.5 \pm 1.5) \times 10^{1}$
494	5200	0.25	1.6×10^{-3}	0.055 ± 0.02	$(2.5 \pm 0.9) \times 10^{2}$
620	14000	0.18	4.3×10^{-4}	0.21 ± 0.05	$(3.6 \pm 0.9) \times 10^{3}$
800	15600	0.11	2.4×10^{-4}	0.15 ± 0.05	$(4.7 \pm 1.6) \times 10^{3}$

[a] From ref 2. [b] C_{electron}, concentration of the solvated electron. [c] R_I, Raman intensity ratio between the water transient and bulk water bands. [d] $f_{\text{resonance}}$, resonance enhancement factor.

measured femtosecond time-resolved absorption following the s → p photoexcitation but did not detect either anisotropy or hole burning in the absorption signal.[14,32]

The polarization measurement of Raman scattering (the Raman depolarization ratio) affords decisive information about the symmetry of the molecular vibration: In the non-resonant case, the totally symmetric vibration gives the depolarization ratio between 0 and 0.75 ($0 \leq \rho < 0.75$), whereas the nontotally symmetric vibrations give the value of 0.75 ($\rho = 0.75$). Moreover, in the case of resonance Raman scattering, the Raman depolarization ratio provides information about the symmetry and degeneracy of the excited state in resonance. For example, when the resonant excited state is nondegenerate and only one component of the transition moment from the ground state is nonzero, the depolarization ratio is known to become 1/3, because only one diagonal component of the Raman tensor (α_{xx}, α_{yy}, or α_{zz}) can have a nonzero value. Therefore, the polarization measurement of resonance Raman scattering can provide unique information about the excited p state of the solvated electron.

Polarized time-resolved resonance Raman spectra of the OH bend region were measured at the delay time of 20 ps and they are shown in Figure 10. Although the quality of the obtained spectra is not good, the transient Raman band due to the OH bending vibration of the solvating water molecules was clearly seen as marked by arrows. It is obvious that the transient Raman band was observed also in the perpendicular spectrum, although the quite low signal-to-noise ratio hindered us from determining the depolarization ratio quantitatively. This demonstrates that the depolarization ratio of the transient resonance Raman band is definitely *not zero*.

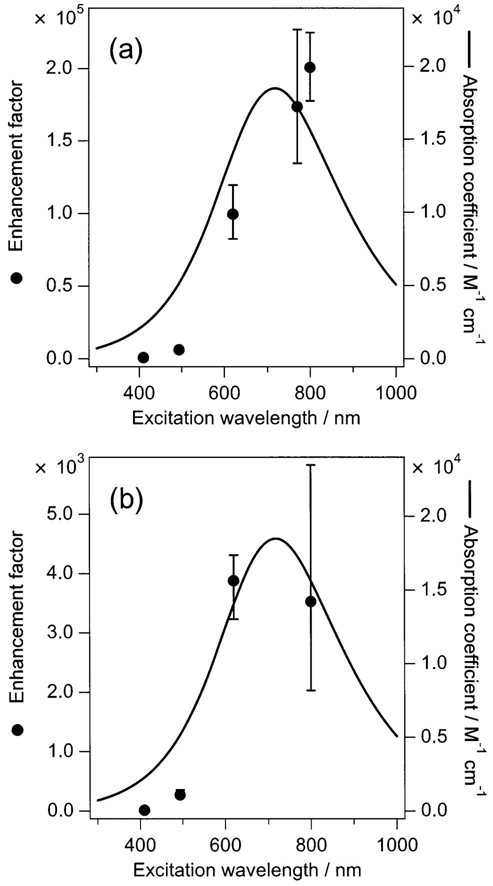

Figure 9. Excitation profiles of (a) the OH bend and (b) the OH stretch bands. The absorption spectrum reported by Jou and Freeman[2] is also shown with solid lines.

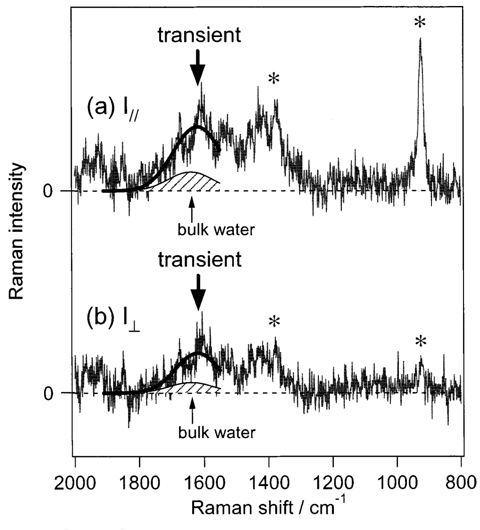

Figure 10. Polarized transient resonance Raman spectra in the OH bend region of a water−acetonitrile mixture (4:1) in the presence of ferrocyanide ion (5×10^{-3} mol dm^{-3}; pump laser, 270 nm; probe laser, 810 nm, delay time, 20 ps). (a) Parallel and (b) perpendicular polarized Raman scattering. The spectrum taken with only pump pulse irradiation and the luminescence signal arising from probe pulse irradiation have been subtracted. The Raman bands of acetonitrile are indicated by asterisks.

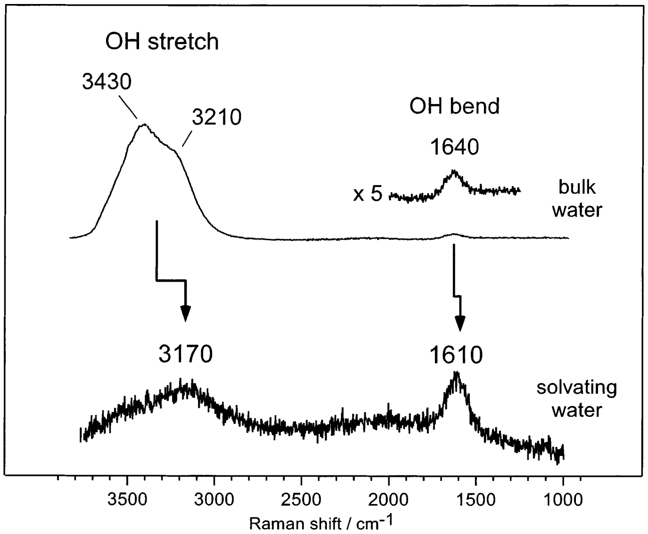

Figure 11. The non-resonance Raman spectrum of bulk water (top; 600 nm excitation) and the resonance Raman spectrum of the water molecules that solvate the electron (bottom; 620 nm excitation).

If the local environment around the electron is isotropic, the three sublevels of the excited p state are degenerate. Then, the p_x, p_y, and p_z states equivalently contribute to the resonance Raman process and the three diagonal components of the Raman tensor (α_{xx}, α_{yy}, or α_{zz}) have the same value. (The Raman tensor becomes isotropic.) This type of the isotropic Raman tensor gives the Raman depolarization ratio of zero ($\rho = 0$). However, the observed Raman depolarization ratio is not zero, which sharply contradicts the above argument based on the degeneracy of the three sublevels. Therefore, the observed nonzero depolarization ratio strongly indicates that the three sublevels of the p state do not equally contribute to the resonance Raman process. In other words, the resonance Raman process seems to "feel" the nondegeneracy of the p_x, p_y, and p_z states, within a time scale of its optical process.

The time scale of the resonance Raman process is equivalent to the dephasing time of the electronic transition. Therefore, it can be estimated from the width of the absorption band. The absorption of the solvated electron is asymmetric and is considered to be broadened due to the nondegeneracy of the three sublevels of the p-state (inhomogeneous broadening). Thus, the apparent bandwidth of the absorption gives the shortest limit of the time scale of the resonance Raman process. The bandwidth of the solvated electron absorption is ~6700 cm^{-1},[2] which corresponds to a time scale (a dephasing time) of 2−3 fs. The observed nonzero value of the depolarization ratio suggests that the nondegeneracy of the three sublevels is "observable" in this short time scale of the Raman process. Assell et al. did not observe any hole burning in their femtosecond absorption experiments, and they concluded that the relaxation among the three sublevels occurs within 80 fs.[14] If their value is adopted as the upper limit, the redistribution time of the three sublevels of the p state can be considered to be in the range of $2-3 \text{ fs} < \tau < 80 \text{ fs}$.

3.6. Raman Spectra of the Local Structure around the Solvated Electron. The present study shows that we can obtain the Raman spectrum of the water molecules that solvate the electron, when we measure Raman scattering under the resonance condition with the s → p transition of the solvated electron. In Figure 11, the resonance Raman spectrum of the "solvated electron" is compared with the spectrum of the bulk water. (To show the Raman spectrum measured with a single detector, we show the "solvated electron" spectrum taken with the 620-nm probe.) Similarity seen between the two spectra indicates that the "solvated electron" spectrum is basically *the spectrum of water*. However, the Raman spectrum of the "solvated electron" is significantly different from the spectrum of the ordinary water in several points. First, the intensity of the OH bend band is much higher than that of the OH stretch band, reflecting the resonance condition. Second, the vibrational frequencies are downshifted compared with the corresponding frequencies of the bulk water. The OH bending frequency is ~30 cm^{-1} lower than that of the bulk water, whereas the OH stretching frequency is downshifted by ~150 cm^{-1} from the average of the anti-symmetric and symmetric OH stretching frequencies of the bulk water. Third, most strikingly, the intensity of the Raman scattering is highly enhanced under this resonance condition. For example, the OH bend band of the solvating water molecules gains the intensity enhancement in the order of 10^5 when the probe wavelength is tuned to the intensity maximum of the absorption band of the solvated electron.

The resonance enhancement as large as $\sim 2 \times 10^5$ is quite large, even compared with the resonance Raman enhancement of ordinary molecules. In fact, it is comparable to the resonance enhancement of β-carotene.[33] This fact strongly suggests very strong interaction between the electron and the water molecules in the first solvation shell. The observed very high resonance enhancement of the solvating water molecules claims that the picture of "an electron in a cavity" is too simple when we consider the vibronic state of the "solvated electron", because the electronic state of the electron and the vibrational state of the solvating molecules are strongly coupled. We should treat the solvated electron in water as a "water cluster anion" in the condensed phase. We think that this is the most important implication of the results of the present resonance Raman study.

The water cluster anion has been intensively studied in the gas phase, in relation to the interest in the solvated electron. Therefore, it is worth comparing the vibrational frequency of the water cluster anion in the gas phase with the frequency of the water transient observed in the present time-resolved Raman study. Johnson and co-workers reported autodetachment spectra of the mass-selected water cluster anions in the gas phase, which corresponds to the IR spectra in the OH stretch region.[17,18] They compared the obtained vibrational spectra with the result of theoretical calculations, and claimed that the water cluster anion has a linear chainlike structure, and the electron is attached at one end of the chain.[17] According to their assignment based on a density functional calculation, the OH stretch frequency of the water molecule that is directly attached to the electron is lower than the stretching frequency of the free OH, but it is higher than the stretching frequency of the hydrogen-bonded OH which makes the backbone of the chainlike structure. It seems that this order of the stretching frequency, ν (free OH) > ν (OH...e) > ν (hydrogen-bonded OH), is not specific to the water cluster anion having a chainlike structure. Actually, other structures have also been suggested by theoretical calculations of the other groups,[19−21] and the vibrational spectra of the several possible conformers have been calculated. In any calculated cluster anion in the gas phase, the OH stretching frequency of the water molecule attached to the electron is higher than that of the hydrogen-bonded OH. This is a sharp contrast to our observation for the solvated electron in the condensed phase. In the observed resonance Raman spectra, the OH stretching frequency of the solvating water molecules is lower than the frequency of the bulk water molecules which are hydrogen-bonded. This means that the electron−water interaction in the condensed phase is much stronger than that in the cluster in the gas phase. Although the structure of the water cluster anions in the gas phase is still controversial, it has been agreed that the stable water cluster anion is the surface state, in which the electron is trapped on the surface of the cluster and it is exposed to the vacuum. In such a surface state, the electron is much more delocalized, compared with the internal state. Undoubtedly, in the condensed phase, the electron is surrounded by the water molecules and hence the "water cluster anion in water" (or the "solvated-electron cluster"), is the internal state. Naturally, the electron is more localized, which results in much stronger interaction between the electron and the water molecules in the first solvation shell. It is noteworthy that theoretical calculations indicated that the OH stretching frequency can be a good indicator of the strength of the O−H...e^- interaction.[19,20] It is highly likely that the difference in the delocalization of the electron between the gas phase and the condensed phase is reflected on the OH stretching frequency.

Finally, we discuss the uniqueness of the frequency shift of the OH bend and OH stretch vibrations observed in the present study. In ordinary hydrogen bonding systems, it is known that the frequency shift of the OH stretching vibration is opposite to that of the OH bending vibration.[34] For example, as the hydrogen bonding strength increases, in usual cases, the OH stretching frequency decreases whereas the OH bending frequency increases. However, both of the OH bending and OH stretching frequencies of the observed water transient are lower than those of the bulk water, which means that the strong interaction with the electron causes downshifts of both of the bending and stretching frequencies. This unique frequency shift looked puzzling for us at the beginning. However, we now consider that these frequency shifts are also consistent with the assignment that the observed transient species is the water molecule that directly solvates the electron.

A simple explanation about the ordinary opposite frequency shift of the OH stretch and OH bend vibrations is described as follows, for a simplified case that an O−H bond is hydrogen-bonded to the neighboring X atom (O−H...X). Concerning the O−H stretching frequency, as the strength of the H...X hydrogen bond increases, the O−H bond strength decreases (and the bond length increases), which causes a downshift of the O−H(...X) stretching frequency. On the other hand, for the O−H bending motion, the hydrogen bond between H and X atoms provides additional restoring force because the bending motion is off-axial motion for the linear O−H...X structure. In other words, the H...X hydrogen bonding acts as "the second spring" for the O−H bending vibration. Thus, even if the O−H bond strength decreases, as the hydrogen bonding strength increases, the force constant for the O−H(...X) bending motion increases with the help of the H...X hydrogen bond. As a result, the O−H(...X) bending frequency shows an upshift. Although this explanation is very simple, it describes the physical background of the opposite shifts of the OH stretching and OH bending frequencies in ordinary hydrogen-bonded systems. Here, we should note that this discussion, especially for the bending vibration, assumes that the X atom is much heavier than hydrogen. It is because the end of "the second spring" needs to be fixed in a space in order that the H...X bonding acts as a restoring force. Obviously, this assumption is not valid for the case of the OH bond that interacts with the electron. In this case, X corresponds to the electron which is very light. Therefore, even if the interaction between the OH bond and the electron is strong, the O−H...e^- interaction does not afford any practical restoring force for the O−H(...e^-) bending motion owing to the lightness of the electron. Thus, it seems that the OH bending frequency does not necessarily show an upshift although the OH stretching frequency exhibits a significant downshift due to the strong O−H...e^- interaction. On the basis of this discussion, we consider that the observed unique frequency shifts is consistent with the assignment that the observed water transient is the water molecule in the first solvation shell, and also it is consistent with the Keavan's type local structure around the electron in which one of the OH bonds of the water molecule is oriented toward the center of the electron.[16] It is considered that the electron is stabilized by the electrostatic interaction between the electron and OH bond dipole in this type of the solvation structure.[19,20]

In the present paper, we reported the observation of the Raman scattering from the local structure around the solvated electron. This observation strongly suggests that the interaction between the electron and the water molecules is so strong that we should consider them together, at least, from the viewpoint of the vibronic state of the local structure. The observed vibrational frequencies suggest a significant structural change induced by the interaction with the electron in the ground state, and the resonance Raman intensity affords information about the structural change induced by the s → p electronic excitation. The polarization measurements provide a clue for discussing the nondegeneracy of the excited p state as well as the time scale of the relaxation. Time-resolved Raman spectroscopy has afforded important data that raise a series of new questions about the solvated electron in water. Further studies, especially theoretical studies, are very desirable in order to rationalize the vibrational data of the solvated electron, which deepens our understanding of the nature of this very fundamental anionic species in the condensed phase.

Acknowledgment. We thank Prof. Mitsuo Tasumi and Prof. Hiroaki Takahashi for stimulating discussions about the vibrational frequencies of the hydrogen-bonded systems. This work was supported by a Grant-in-Aid for Scientific Research (B) (No. 13440183) from Japan Society for Promotion of Science (JSPS).

References and Notes

(1) Hart, E. J.; Boag, J. W. *J. Am. Chem. Soc.* **1962**, *84*, 4090.

(2) Jou, F.-Y.; Freeman, G. R. *J. Phys. Chem.* **1979**, *83*, 2383.

(3) Schnitker, J.; Motakabbir, K.; Rossky, P. J.; Friesner, R. *Phys. Rev. Lett.* **1988**, *60*, 456.

(4) The other possibility of the assignment of this broad absorption band has been proposed by theoretical calculations. See the following papers: Muguet, F. F.; Gelabert, H.; Gauduel, Y. *J. Chim. Phys.* **1996**, *93*, 1808. Sobolewski, A. J.; Domcke W. *J. Chem. Phys. A* **2002**, *106*, 4158.

(5) Nikogosyan, D. N.; Oraevsky, A. A.; Rupasov, V. I. *Chem. Phys.* **1983**, *77*, 131.

(6) Miyasaka, H.; Masuhara, H.; Mataga, N. *Chem. Phys. Lett.* **1983**, *98*, 277.

(7) Migus, A.; Gauduel, Y.; Martin, J. L.; Antonetti, A. *Phys. Rev. Lett.* **1987**, *58*, 1559.

(8) Gauduel, Y.; Pommeret, S.; Antonetti, A. *J. Phys. Chem.* **1993**, *97*, 134.

(9) Laenen, R.; Roth, T.; Laubereau, A. *Phys. Rev. Lett.* **2000**, *85*, 50.

(10) Vilchiz, V. H.; Kloepfer, J. A.; Germaine, A. C.; Lenchenkov, V. A.; Bradforth, S. E. *J. Phys. Chem. A* **2001**, *105*, 1711.

(11) Kambhampati, P.; Son, D. H.; Kee, T. W.; Barbara, P. F. *J. Phys. Chem. A* **2002**, *106*, 2374.

(12) Son, D. H.; Kambhampati, P.; Kee, T. W.; Barbara, P. F. *J. Phys. Chem. A* **2001**, *105*, 8269.

(13) Son, D. H.; Kambhampati, P.; Kee, T. W.; Barbara, P. F. *Chem. Phys. Lett.* **2001**, *342*, 571.

(14) Assel, M.; Laenen, R.; Laubereau, A. *Chem. Phys. Lett.* **2000**, *317*, 13.

(15) Reid, P. J.; Silva, C.; Walhout, P. K.; Barbara, P. F. *Chem. Phys. Lett.* **1994**, *228*, 658.

(16) Keavan, L. *Radiat. Phys. Chem.* **1981**, *17*, 413.

(17) Ayotte, P.; Weddle, G. H.; Bailey, C. G.; Johnson, M. A.; Vila, F.; Jordan, K. D. *J. Chem. Phys.* **1999**, *110*, 6268.

(18) Bailey, C. G.; Kim, J.; Johnson, M. A. *J. Phys. Chem.* **1996**, *100*, 16782.

(19) Tsurusawa, T.; Iwata, S. *Chem. Phys. Lett.* **2000**, *315*, 433.

(20) Iwata, S.; Tsurusawa, T. Electronic and geometric strucures of water cluster complexes with a group 1 metal atom: Electron hydrogen bond in the OH{e}HO structure. In *Adv. Met. Semicond. Clusters* **2001**, *5*, 39.

(21) Kim, J.; Park, J. M.; Oh, K. S.; Lee, J. Y.; Lee, S.; Kim, K. S. *J. Chem. Phys.* **1997**, *106*, 10207.

(22) Mizuno, M.; Tahara, T. *J. Phys. Chem. A* **2001**, *105*, 8823.

(23) Tauber, M. J.; Mathies, R. A. *J. Phys. Chem. A* **2001**, *105*, 10952.

(24) Tauber, M. J.; Mathies, R. A. *Chem. Phys. Lett.* **2002**, *354*, 518.

(25) Shimojima, A.; Tahara, T. *J. Phys. Chem. B* **2000**, *104*, 9288.

(26) Fujino, T.; Tahara, T. *J. Phys. Chem. A* **2000**, *104*, 4203.

(27) Hirata, Y.; Murata, N.; Tanioka, Y.; Mataga, N. *J. Phys. Chem.* **1989**, *93*, 4527.

(28) Buxton, G. V.; Greenstock, C. L.; Helman, W. P.; Ross, A. B. *J. Phys. Chem. Ref. Data* **1988**, *17*, 513.

(29) Prezhdo, O. V.; Rossky, P. J. *J. Phys. Chem.* **1996**, *100*, 17094.

(30) Albrecht, A. C. *J. Chem. Phys.* **1961**, *34*, 1476.

(31) The frequency resolution of the spectra taken with 494-nm probe pulse is worse than that taken with the other probe wavelength owing to the broadness of the excitation line.

(32) In an earlier femtosecond time-resolved absorption measurement, Barbara and co-workers reported that the anisotropy was observed. See ref 15.

(33) Tasumi, M. Resonance Raman Scattering I. General aspects. In *Laser-Raman Spectroscopy and Its Applications*; Shimanouchi, T., Tasumi, M., Harada, I., Eds.; Nankodo: Tokyo, 1977.

(34) Falk, M. *Spectrochim. Acta* **1984**, *40A*, 43.